



Assessment of Operational Reliability for eVTOL Vehicle Design

Hajar Mali*, Jouwairia Ahabchane[†], Evan D. Harrison[‡], Jiacheng Xie[§], Dimitri N. Mavris[¶]
Georgia Institute of Technology, Atlanta, GA, 30332

With the advent of electric vertical takeoff and landing (eVTOL) vehicles, a new era of efficient and sustainable air travel has been promised. At the core of this pivotal shift lies operational reliability which depends on technological advancements, regulatory standards, and effective maintenance and safety practices. A proper assessment of operational reliability is of critical importance for the successful integration of these novel vehicles while gaining public trust and acceptance. The objective of this work is to assess the impact of potential vehicle hazards occurring whilst in flight, as they are susceptible of compromising the completion of eVTOL missions or jeopardizing the integrity of the vehicle and/or putting the safety of its passengers at risk. A parametric tool is developed allowing a comprehensive evaluation of the operational reliability of different vehicle configurations by tracking and calculating different time metrics of interest. These metrics help formulate more efficient maintenance schedules, extending the service life of various parts as well as ensuring both the integrity of the vehicle and minimizing risks related to downtime, delays, flight cancellations, and safety concerns.

I. Nomenclature

t = time
 β = shape parameter of Weibull distribution
 η = scale parameter of Weibull distribution
 λ = failure rate

II. Introduction

As urban areas continue to expand and grapple with escalating traffic congestion and population density, the concept of urban air mobility (UAM) has gained traction rapidly in recent years. Within this emerging market, the technology of electric vertical take-off and landing (eVTOL) vehicles has seen rapid development over the past decade. In the field of novel technologies, reliability must be rigorously tested and quantified, especially for those that have a substantial influence on public safety and environmental sustainability. This is more important for cutting-edge technologies that have the potential to revolutionize urban air transportation. Operational reliability in the context of eVTOL technology is multifaceted, encompassing crucial elements such as design, maintenance, environmental impact, and quality assurance. The synthesis of these factors provides a holistic approach to safety and reliability, ensuring that eVTOLs can meet stringent operational standards and integrate seamlessly into urban environments. The economic implications of eVTOL reliability extend beyond operational efficiency, influencing company valuations, market acceptance, and consumer trust—factors that are critical to the long-term success of eVTOL initiatives.

Necessitated by the unique demands of eVTOL operations, this paper proposes a method to systematically evaluate the eVTOL maintenance strategies from the perspectives of operational reliability. By leveraging physics-based modeling and simulation, particularly through stochastic modeling with Abridged Petri Nets, this study aims to predict and refine maintenance schedules based on dynamic operational data. Furthermore, the economic ramifications of maintenance decisions are assessed through the quantification of key performance indicators such as Mean Time to Repair (MTTR), Mean Time to Failure (MTTF), Maintenance Recovery Period (MRP), Maintenance-Free Operating Period (MFOP), and Mean Time Between Failures (MTBF).

*Graduate Research Associate, Aerospace Systems Design Laboratory

[†]Graduate Research Associate, Aerospace Systems Design Laboratory

[‡]Senior Research Engineer, Aerospace Systems Design Laboratory, and AIAA Member

[§]Research Engineer II, Aerospace Systems Design Laboratory, and AIAA Member

[¶]Georgia Tech Distinguished Regents Professor and Director of ASDL, AIAA Fellow

III. Literature Review

Given the current scarcity of data and limited operational experience with eVTOL aircraft, a practical starting point for their development is to simulate their novel configurations using existing airplanes and helicopters. By drawing parallels to these well-understood platforms, informed assumptions can be made, and an initial framework for eVTOL operations can be designed. This approach enables leveraging existing knowledge and methodologies to better understand the specific characteristics and potential challenges associated with eVTOL technology, thereby laying the groundwork for more accurate and effective design, testing, and implementation processes.

A. Helicopter and Airplane Failure Modes

Raigoza et al. [1] analyzed and compared incident data from 2015, collected from the National Transportation Safety Board (NTSB), between helicopters and airplanes in the United States. The analyzed dataset consisted of a total of 510 airplanes and 59 helicopters. This effort aimed to identify the failure modes of each aircraft while highlighting their similarities. Table 1 shows that the top three contributing failures are similar for both aircraft types, with the most common failure mode being due to human error, which accounts for 56% of helicopter failures and 57% of airplane failures. The second and third failure modes are engine failure and failure due to environmental factors and they also significantly contribute to incidents for both aircraft categories. Consequently, these observed patterns suggested that the nature of failure may be independent of the aircraft type. This implies that eVTOLs could potentially experience failure mode contributions that are similar, to some extent, to airplanes and helicopters. Therefore, the failure modes observed in conventional aircraft and rotorcraft can serve as a valuable starting point for the identification and assessment of eVTOL failures and their safety and operational implications.

Table 1 Helicopter and airplane failure modes and rates (data from Ref. [1])

Failure mode	Helicopter rate	Airplane rate
Engine Failure	3%	2%
Unknown	3%	5%
Control	3%	2%
Material Fatigue	5%	2%
Rotor	9%	5%
Environmental	9%	8%
Engine Failure	12%	20%
Human Error	56%	57%

B. Expected Similarities and Differences between eVTOL and Helicopter / Fixed-Wing Aircraft

Kinjo [2] highlighted the key differences between helicopter and eVTOL to better understand the implications of their differences in terms of design and operation. eVTOL aircraft consist of multiple rotors driven by electric motors that are mainly powered by batteries, as opposed to helicopters, which rely on a single large rotor propelled by a fuel-powered engine. The multiple rotors in eVTOL configurations increase redundancy and enhance their overall robustness. Consequently, if one of the rotors fails, the remaining rotors could take over and compensate for the failure by adjusting their power output distribution. Moreover, the shift to electric propulsion in eVTOLs leads to reduced noise generation compared to helicopters, with an anticipated noise level 75% lower than that of helicopter [2]. Su et al. [3] explored multiple eVTOL configurations and evaluated their strengths and limitations in terms of their performance and operational suitability. Multi-rotor designs were deemed more suitable for short-range missions as they are constrained by rotor speed limits. In contrast, lift+ cruise and vectored thrust designs were found better suited for long-distance flights due to their fixed-wing design similarities. Ugwueze et al. [4] further substantiated this claim by conducting a range sensitivity study that confirmed the mission-dependent efficiency trade-offs between the wingless and powered lift configurations. Furthermore, Liu et al. [5] conducted a comprehensive CFD analysis confirming hover as the most important limiting phase in terms of power requirements and highlighting the significant rotor/airframe aerodynamic interactions experienced by lift+cruise configurations during hover. Additionally, the transition towards eVTOL vehicles

eliminates complex rotating mechanisms and fuel systems, making the overall aircraft structure much simpler, which in turn is expected to reduce maintenance costs. Helicopter maintenance costs are estimated to contribute to 60% of the overall operational expenses. In contrast, eVTOL maintenance costs are expected to be lower with an approximate contribution of 20% of operational costs, as estimated by the US-based company Uber Technologies [6]. Cheng et al. [7] developed a cost model focusing on powertrain modeling to optimize the overall cost per eVTOL mission. The analysis showed that the two main cost drivers were battery cost and pilot cost, and suggested cost minimization strategies such as autonomous driving, reduction in battery manufacturing costs, and enhanced battery life cycle.

C. Helicopter Accident Rates

According to the U.S. Helicopter Safety Team (UHST) Monthly Safety Report [8], the rate of fatal helicopter accidents between the years 2020 and 2024 is equal to 0.62 per 100 000 flight hours. This number exceeds the goal set for 2025 to reduce fatal accident rates to less than 0.55. Between 2013 and 2017, the yearly total number of helicopter accidents was 127 on average, and the total number of fatal accidents was around 21 on average [9]. Moreover, these values have been declining each year over that time frame, as shown in Table 2. The major failure modes contributing to these accidents are mainly pilot error, mechanical failure, or aircraft collision. eVTOLs will carry out novel missions and operate at low altitudes in urban areas, which implies that new accident or failure scenarios can be expected.

Table 2 US helicopter accidents between 2013 and 2017 (data from Ref. [9])

Year	Total accidents	Total accident rate	Fatal accidents	Fatal accident rate
2017	121	3.55	20	0.59
2016	108	3.45	17	0.54
2015	121	3.67	17	0.52
2014	138	4.26	21	0.65
2013	146	4.95	30	1.02

An analysis of 698 helicopter accidents between 2005 and 2015 was conducted to identify the correlation between helicopter accidents and maintenance/inspections [10]. Figure 1 shows the distribution of flight hours between helicopter maintenance/inspection and accidents. A significant percentage of accident occurrences are observed right after maintenance and inspection interventions. For instance, within the first 10 hours of flight, around 21.5% of accidents occurred with a 95% confidence interval between 18% to 24%. The percentage of accidents keeps decreasing, referred to as infant mortality in reliability engineering. The values start to level off after 70 flight hours and before exceeding the 100-flight-hour mark, known as the constant failure rate phase. Beyond the 100-flight-hour mark, the percentage of accidents suddenly drops. During this last phase, the helicopters typically operate under the Approved Aircraft Inspection Program (AAIP) or the Continuous Airworthiness Maintenance Program (CAMP). Two additional types of maintenance and inspections are set in place: the 100-hour and the annual inspection [10].

Given the operation of eVTOLs in large numbers over urban areas and in such proximity to the ground, the UAM corridor is expected to experience congestion and increased air traffic, which is susceptible to increase the likelihood of collision occurrences. The novel configurations of these vehicles, as well as the level of redundancy they contain, can induce new failure points and failure modes that could potentially differ in terms of propagation or containment behavior compared to conventional aircraft. Consequently, an analysis of the operational reliability of these novel configurations is crucial to better understand their behavior and quantify their operational reliability and safety implications. Furthermore, the limited mission durations and the rate of demand of air mobility services over those limited distances can also have a significant impact on eVTOL operations and their economic viability.

IV. Modeling and Simulation of eVTOL Operations

Risk analysis is crucial in vehicle design as it ensures that safety and quality requirements are met and maximizes confidence and trust in the design. Various modeling and simulation techniques can be employed to capture the reliability and risks associated with the system under test. The relevance and accuracy of the results of such analysis are highly dependent on the type of data used, whether it is sourced from experiments, simulations, databases, or expert opinions.

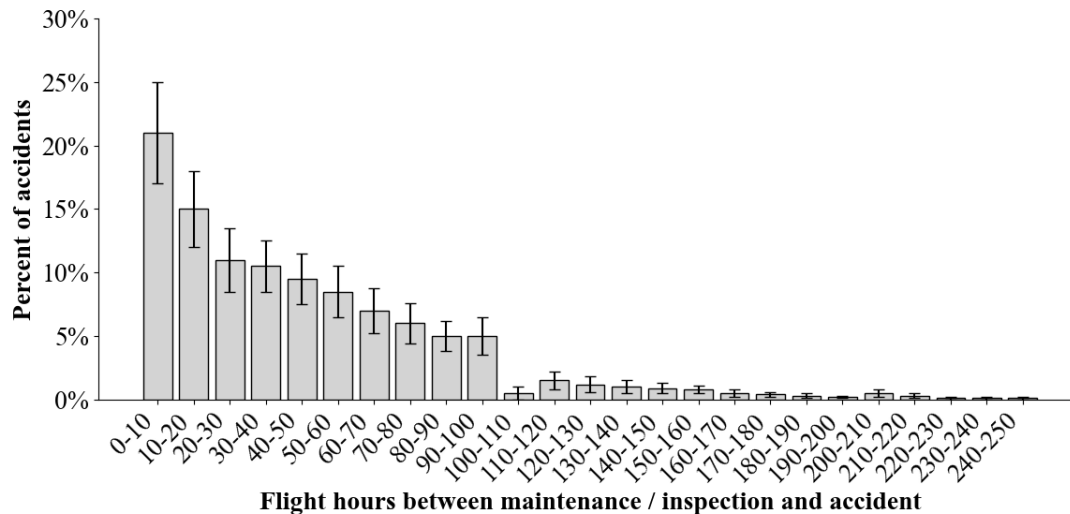


Fig. 1 Distribution of flight hours between helicopter maintenance/inspection and accidents (data from Ref. [10])

However, data can be scarce, incomplete, inaccurate, or simply outdated, limiting the reliability of the results and conclusions. Since eVTOL aircraft are novel concepts but have not yet been in operation, relevant operational data is limited. In addition, competing companies are keeping their design details as proprietary data, making access to operational data even more challenging. Consequently, similarities with traditional aircraft and helicopters are leveraged to develop the necessary assumptions and estimations to create an initial framework that can eventually be adapted to the desired eVTOL specifications once the data are available.

Several methods, both qualitative and quantitative, can be employed for reliability assessment, including but not limited to:

- **Fault Tree Analysis (FTA):** a graphical diagram summarizes all the possible combinations of events that can lead to a specific failure.
- **Event Tree Analysis (ETA):** an extension of FTA analyzes the potential outcomes and consequences specific to a starting event.
- **Monte Carlo Simulation (MCS):** random scenarios are generated based on different combinations of input parameters and simulated to assess the reliability of the system under test.
- **Failure Modes and Effects Analysis (FMEA):** identification and assessment of different failure modes and their effects at both system and sub-system levels.
- **Failure Modes and Effects and Criticality Analysis (FMECA):** a criticality analysis such that the criticality of each failure mode is quantified using a Risk Priority Number (RPN). This number is the product of three indicators: severity indicator (S) refers to the seriousness of the failure; occurrence indicator (O) tells the frequency of the failure; and detection indicator (D) represents the likelihood that a failure is not detected before it causes serious damage.
- **Markov Chains:** a robust framework for modeling system reliability by allowing the estimation of system states and their transitions over time while capturing the probabilistic nature of failures and repairs.
- **Petri-Nets:** a graphical and mathematical modeling tool useful for describing and studying information processing systems characterized by primarily stochastic activity.

In the context of maintenance reliability modeling, Petri-Nets offer a flexible and intuitive approach to represent dynamic systems. They are well-suited for scenarios involving dependencies between component failure rates, varying distribution characteristics, and system reparability. Petri-nets help in visualizing and analyzing system behavior, enabling the assessment of system performance and the identification of potential improvements in system reliability. Moreover, they can capture both static and dynamic behaviors, support fault detection and isolation, and provide a clear representation of system behavior. Unlike Markov Chains, which are limited by their single-step transition structure and strictly sequential state progression, Petri Nets enable arbitrary connections between system states and allow the incorporation of conditional logic beyond simple transition probabilities.

A. Petri-Nets Structure

The methods outlined above can be employed interchangeably or in combination. In this work, the modeling technique of choice is Petri-Nets in conjunction with Monte Carlo Simulation. This captures the inherent stochastic nature of UAM flights due to operation at low altitudes and densely populated areas, demand uncertainty, and system reliability. This approach simulates specific events such as failure occurrences, scheduled and unscheduled maintenance interventions, and inspections. The model is represented as a hierarchical Petri-Net with three distinguishable levels: system level, subsystem level, and component level. The system-level model pertains to the eVTOL operation, including the mission phases, the duration of each phase, the potential maintenance interventions (scheduled and unscheduled maintenance activities), the battery charging and battery replacements, and inspections (including scheduled inspections and pre-flight and post-flight inspections). The subsystem-level model encompasses two main subsystems: the battery subsystem and the propulsion subsystem. The component-level model captures the failure occurrences associated with physical components and their impacts on the subsystem and system reliability and operation.

A typical Petri-Net is composed of four elements: places indicating the system states, tokens indicating the system, arcs indicating the tokens' directions of movements, and transitions indicating the time delay, which can be fixed or follow a specific distribution such as Weibull, lognormal, or uniform. The software used is Abridged Petri-Nets (APN) developed by Volovoi [11]. This Petri-Net variant simplifies the structure and reduces it to three elements by merging the arcs and transitions, thus providing a clearer graphical representation of the model as shown in Fig. 2.

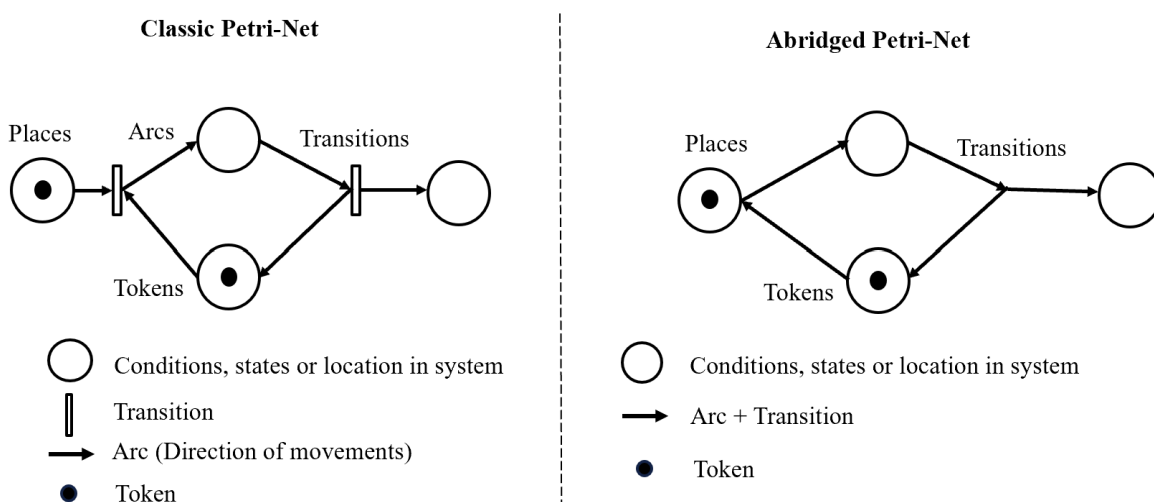


Fig. 2 Structure of a classic Petri-Net and Abridged Petri-Net

B. Technical Approach Overview

Prior to setting up the model capabilities, certain assumptions need to be specified. This work considers that all necessary infrastructures to enable and support eVTOL operations are set and all maintenance and inspection activities can be carried out in landing locations. This entails that all necessary equipment, parts, and crew members are available at all times and at all locations. The developed model is applicable to a specific mission profile (takeoff, climb, cruise, descent, loiter, and landing) with user-specified durations for each mission phase.

The overall approach used to model eVTOL operations and assess their operational reliability is described through Fig. 3. To properly capture an eVTOL operation, three main categories of inputs are defined:

- **Vehicle characteristics** include the vehicle configuration to be analyzed and the level of redundancy of the subsystems being modeled (i.e., number of battery packs and number of rotors).
- **Mission Profile** describes the mission phases to be flown and the duration of each phase. The mission profile considers the battery charging time and the frequency of battery replacements.
- **Maintenance and Inspections** consist of modeling the prescribed cadence of scheduled maintenance and inspections.
- **Failure Modeling** identifies the failure triggers at the component level that will affect the subsystem-level function and the system-level operation. Upon failure occurrence and detection, the eVTOL conducts the necessary type of

landing, passengers disembark from it, and then it undergoes unscheduled maintenance before taking in more flights.

These inputs are provided to the modeling and simulation environment from which the outputs are collected as raw data within a MATLAB file. This file is then processed using a Python script designed to properly track and calculate the desired metrics of interest for this analysis.

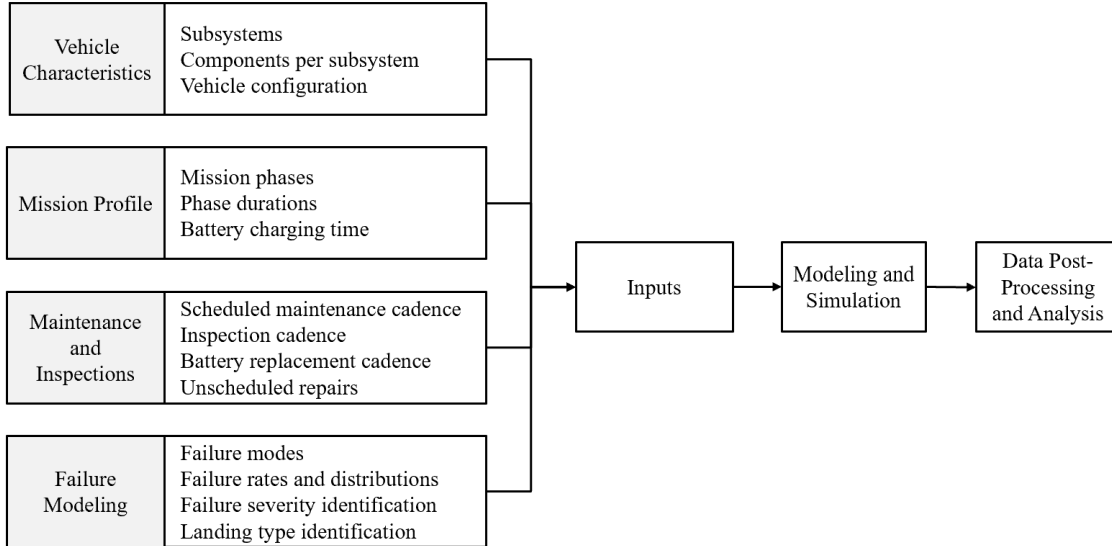


Fig. 3 Technical approach overview

C. Physical Decomposition of the System

Within an eVTOL system, there are several subsystems, each with distinct components and functions. The propulsion subsystem includes the electric motors and propellers, while the controls subsystem is comprised of the flight control software, actuators, and sensors. The battery subsystem encompasses the battery cells, battery management system, and wiring. The structural subsystem refers to the airframe, wings, rotors, and landing gear or skids. As for the communication and navigation subsystem, it typically consists of data links, communication protocols, and GPS. Additionally, eVTOLs are typically equipped with safety subsystems including elements such as parachutes and emergency landing gear deployment.

As a proof of concept, this paper implements the battery subsystem and the propulsion subsystem to illustrate the proposed method, but the same process can also be applied to other subsystems for a more holistic analysis.

In this paper, the behaviors of battery and propulsion subsystems and their impacts on the overall operation and reliability of eVTOL aircraft are modeled and analyzed. Each subsystem is further decomposed into its primary components. The battery subsystem is comprised of the battery management system (BMS), battery packs, and internal wiring. The propulsion subsystem consists of the power management system (PMS), motors, inverters and controllers, rotors, and external wiring.

D. Failure Rates and Failure Distributions

Failure rates can change with respect to time as they can decrease, increase, or remain constant over time. The bathtub curve is a graphical representation of the failure rate over time for many products and systems. It is a combination of a decreasing failure rate for early or “infant mortality” failures, a constant failure rate during the system’s useful life, and an increasing failure rate as the system approaches wear-out failures, as shown in Fig. 4.

To model failure behaviors, various distributions can be used, including but not limited to lognormal, uniform, exponential, χ^2 , Weibull, binormal, and Fisher-Snedecor distributions [12]. In this paper, Weibull distributions are used in modeling and simulation of failure occurrences during eVTOL operations due to their flexibility and ability to capture various failure behaviors using the shape parameter which determines the failure rate trend over time, and the scale parameter which sets the characteristic life scale, indicating the time by which a specific percentage of failures

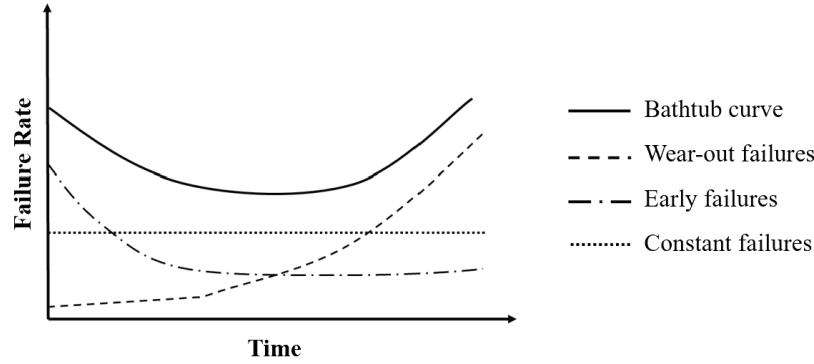


Fig. 4 Failure rate behavior with respect to time

is expected to occur. The failure triggers follow a Weibull distribution with different settings for the scale and shape parameters to approximate the behavior and failure rate of each component failure mode. The failure rate function $\lambda(t)$ for a system following the Weibull distribution can be expressed in terms of the distribution's scale parameter η representing the characteristic life, and shape parameter β indicating the failure rate behavior over time. The formula for the failure rate at any given time t is given by:

$$\lambda(t) = \frac{\beta}{\eta} \left(\frac{t}{\eta} \right)^{\beta-1} \quad (1)$$

This formula captures how the failure rate varies with time for different values of β and η , providing insights into the reliability and longevity of the system under analysis [13].

E. Identification of Failure Consequences, Severity, and Mission Outcome

Before each flight, the vehicle undergoes a pre-flight check to decide if the initiation of the mission is safe and can start on time ("Go"), or if it is conditioned by certain operational changes or maintenance actions that should take place beforehand which would be susceptible to causing delays ("Go if"), or if the system needs heavy repairs which would certainly lead to significant delays if not a complete cancellation of the mission ("No go") [14]. These frequent inspections ensure the safety of the operations and help detect and predict certain failure modes before they can propagate throughout the system and lead to major complications or accidents. Nonetheless, unexpected failure can occur during operation, whether due to an exterior event or an internal error within a component or subsystem. Once the failure is detected, the vehicle will proceed to activate its redundant systems and adjust its reconfigurable systems to contain the failure and ensure that mission safety is not compromised. If the issue is successfully contained, the vehicle will keep monitoring the failure status while continuing the flight toward its destination. If the issue is not properly contained or if it is propagating, the vehicle will land at the nearest vertiport. If the failure is of extreme severity, then the vehicle will head towards any clear location for an emergency landing; otherwise it may make its way toward the nearest maintenance hub for inspection and repair before it continues its mission or transfer to a different vehicle to ensure passenger safety and mission completion with no major delays.

To assess the operational reliability of a vehicle, it is necessary to identify the potential failure modes corresponding to its subsystems and components, as well as determine the consequences of each possible failure. This enables determining failure rates, failure severity, and failure propagation/containment throughout the whole system. The success of an eVTOL mission depends on whether the vehicle is able to reach its destination without any substantial damage or failure and without any harm to its passengers. The eventual landing location of the eVTOL is primarily dictated by the type of component failure mode triggered, its impact on the subsystem function, and its severity on both subsystem and system levels. In this paper, the vehicle is considered to have enough redundancy that would prevent the propagation of the failure because the malfunctioning components are typically isolated while the functions of the remaining components are adjusted and the backup subsystems are activated to ensure safe landing.

Failure severity can be classified into five categories based on their safety implications [15], as shown on Table 3. They can range from catastrophic severity, which highly compromises vehicle integrity and passenger safety, such as risking a fire or explosion. The other extreme is insignificant severity, which does not impact the system's safety or

functionality, such as having a malfunction in the entertainment screens on board. A maximum probability per flight hour can be allocated to each severity level, as depicted by Table 3. In this paper, it is assumed that the design of the operating eVTOL satisfies the ARP-4761 safety requirements.

Table 3 Failure condition severity as related to probability objectives and assurance levels [15]

Failure severity	Development assurance level	Maximum occurrence per flight hour
Catastrophic	A	10^{-9}
Hazardous (severe major)	B	10^{-7}
Major	C	10^{-5}
Minor	D	10^{-3}
No safety effect	E	–

V. Metrics of Interest

To evaluate the operational reliability of the vehicle, various metrics are tracked. Some are time-based metrics, such as maintenance-free operating period, mean time to failure, mean time between failures, flight time, and downtime. Others quantify the number of failures, their severity level, and the associated landing scenarios.

Maintenance Free Operating Period (MFOP) is defined as the time during which the vehicle is operational and is free from any maintenance activities. During this period, the vehicle should carry out all its designated missions without any interruptions caused by subsystem defects or limitations [16]. The profit an eVTOL operator can make is tied to the maintenance-free operating period. The objective is to increase the MFOP value with a high level of certainty by improving the reliability of subsystems and components. In this paper, MFOP is measured from the take-off place to the next occurrence of either scheduled maintenance or unscheduled maintenance, whichever event occurs first.

Mean Time To Failure (MTTF) is a key reliability metric used to quantify the average duration for which the eVTOL remains operational before encountering a malfunction that leads to unscheduled maintenance. This metric provides insight to the vehicle’s performance and the frequency of required unscheduled maintenance interventions. MTTF is calculated as the time measured from takeoff to the next recorded failure.

Mean Time Between Failure (MTBF) is also used to determine the average duration a vehicle is operational before experiencing a failure. It indicates the time interval between two consecutive failures of the system under normal operating conditions, serving as a key indicator of the system’s reliability and performance. In this study, for missions that have multiple failure occurrences, only the first recorded failure is considered for MTBF calculation.

Flight time is the total duration the aircraft executing the flight operation. It includes the time from takeoff to landing. Total downtime is the period during which the eVTOL is not operational due to maintenance events. It is divided into two categories: planned downtime, which includes the duration spent in scheduled maintenance, and unplanned downtime, which accounts for the time spent in unscheduled maintenance resulting from failure events.

The number of failures is recorded for the subsystems and their components, as well as their severity levels. Additionally, landing scenarios corresponding to each failure are tracked to determine the percentage of landings that occurred at destination, at a closer vertiport, or as emergency landings.

VI. Model Demonstration

This work models and simulates three different vehicle configurations incorporating design differences through the number of components and charging time to evaluate their operational reliability. The reliability of components of the same kind is assumed to be the same for all configurations. Table 4 lists the design characteristics corresponding to the three leading eVTOL models currently under development. This section provides an overview of how each of these systems is divided into three main levels that are implemented in APN software.

Table 4 Key specifications of three use-case eVTOL aircraft

Metric	eVTOL A	eVTOL B	eVTOL C
Maximum takeoff weight (lb)	7000	5300	2400
Number of rotors	12	6	12
Number of electric motors	12	6	12
Number of inverters	12	6	12
Number of battery packs	6	4	4
Charging time (min)	10	8	15

A. Use Case Formulation

The vehicle configuration of eVTOL A is used below to illustrate the different building blocks of the model. The model is divided into three main levels: the mission petri-net, subsystem-level sub-nets, and component-level sub-nets corresponding to each subsystem.

1. Mission Petri-Net

Figure 5 depicts the mission petri-net in which the eVTOL token goes through different flight phases: takeoff, climb, cruise, descent, potential loiter, and landing. Specific time durations are allocated to each flight phase, as shown in Table 5. Flight demand is modeled as a lognormal distribution with a mean of 1 hour and a standard deviation of 0.55 hour. Three types of landings can be detected in the mission net and they depend on both the component-level and subsystem-level sub-nets. Following passenger disembarkation, if no failure is detected, the eVTOL token will be pushed through the pre-flight inspection and battery charging prior to entering standby status for the upcoming flight. Routine interventions, including scheduled maintenance, inspections, and battery replacements, are incorporated at the system level and they are only triggered after specific flight hours: 50, 100, and 1000. Since the simulation time accounts for both ground and flight time, a counter is needed to keep track of these individual flight times to trigger the corresponding intervention and re-initialize the counter upon completion. Each counter is designed as a token that turns on whenever the eVTOL takes off in the mission net and pauses every time it lands, as shown in Fig. 6. The “Clock on” place in the counter net has an active aging property that allows the accumulation of time spent by the token in that specific place. Consequently, time is continuously adding up whenever the eVTOL is in flight. Once the accumulated flight time reaches the threshold of a specific intervention, the transition between “Clock on” and the leftmost place labeled with the corresponding threshold is triggered, and the token is fired to this new place. These counters are connected to the mission net through "enablers" and "inhibitors" which are structures that allow the conditioning and synchronization of different events across different nets. These connectors are used such that the eVTOL in the mission net is pushed towards the intervention that reached its threshold before the next flight. Once the intervention is complete, the age of the counter token is reset to zero, and it is pushed back to the “Clock off” position.

Table 5 Mission phases and durations

Flight phase	Duration (min)
Takeoff	1
Climb	2
Cruise	6
Descent	2
Loiter	2
Landing	1

Unlike routine interventions, unscheduled maintenance is independent of flight time. It is initiated after the disembarkation whenever any type of failure has been detected during flight, and it has to be completed before going

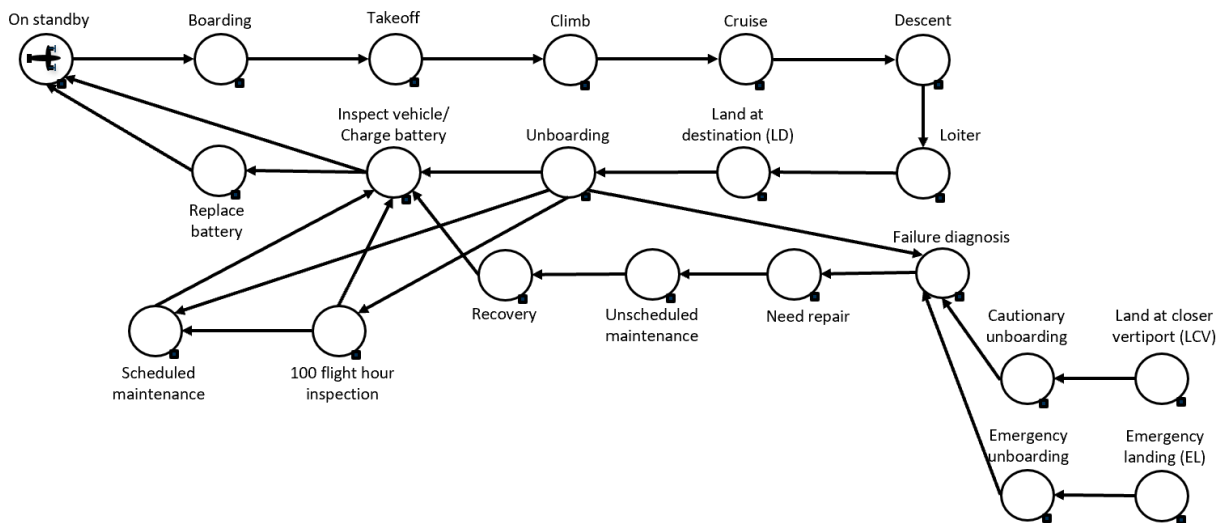


Fig. 5 Mission petri-net structure

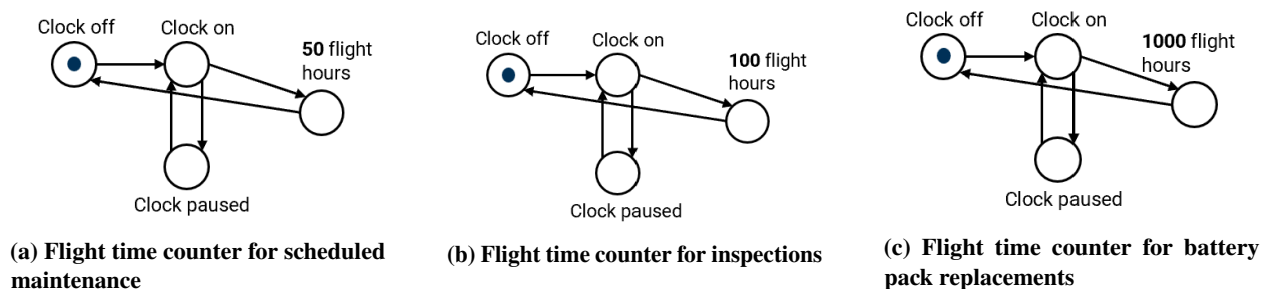


Fig. 6 Flight time counters for routine interventions

through the pre-flight inspection and entering standby mode. Unscheduled maintenance activities go through three main stages: failure diagnosis, repair, and recovery. The duration of the failure and recovery stages is considered to be fixed, with the former taking one hour and the latter taking three hours. In contrast, the actual repair time is variable as it depends on the failure types and the number of failures that have occurred. In other words, the eVTOL token can only move out of the “Unscheduled Maintenance” place in the mission net if every failed component has been repaired at the component-level sub-net. Table 6 depicts the repair duration allocated to each component failure mode. The model assumes that enough crew members are available at all times, allowing all repairs to be initiated simultaneously.

2. Subsystem Sub-Net

This work models two subsystems: the battery subsystem and the propulsion subsystem. The former contains four component types: battery management system (BMS), backup BMS, battery packs, and internal wiring. A total of four failure modes are considered, two of which are related to the battery packs: overdischarging failure and internal short circuit failure as shown in Table 7. The propulsion subsystem contains five component types: propulsion management system (PMS), backup PMS, motors, inverters, rotors, and external wiring. A single failure mode is modeled for each component type. At the component level, each failure mode is allocated an approximated failure rate based on its expected severity level, ranging from level 1 (lowest component severity) to 4 (highest component severity). An extra level of severity is considered when having multiple components of the same type, i.e., battery packs, rotors, motors, inverters, and controllers. Namely, if more than one component of the same type fails, then the severity is increased by one level. In the event of BMS failure, the backup BMS is typically activated to prevent any loss of functionality. However, should the backup fail as well, the severity of BMS failure increases by one level. At the subsystem-level,

Table 6 Repair duration and age renewal factors for component failures

Failure mode	Duration (h)	Age renewal factor
<i>Battery subsystem</i>		
BMS failure	1.0	0.95
Battery pack failure	2.0	0.95
Wiring failure	0.5	0.00
<i>Propulsion subsystem</i>		
PMS failure	2.0	0.95
Motor failure	1.0	0.95
Inverter failure	1.5	0.95
Rotor failure	1.5	0.95
Wiring failure	0.5	0.00

the sub-net shown in Fig. 7 combines the component severity levels of active failure modes to identify the severity at the subsystem-level by setting it to the highest active component severity. This logic cascades up to the system level to identify the overall failure severity state on the vehicle as a whole. If the system severity is minor or major, then the eVTOL is considered to be able to successfully contain the failure and continue to its destination. However, if the severity is hazardous, failure containment may only be partial, thus posing a risk to the vehicle integrity and passenger safety. Consequently, the eVTOL is expected to land at a closer vertiport out of precaution. Otherwise, should the severity be of high risk and potentially of catastrophic impact, the eVTOL is expected to immediately find a clear space to conduct an emergency landing to prevent any further failure propagation and aggravated damage.

Table 7 Component failure settings for the battery and propulsion subsystems

Failure mode	Severity level	Failure distribution	Failure rate	Shape β	Scale η (h)
<i>Battery Subsystem</i>					
BMS failure	Level 2	Weibull	10^{-5}	2	447
Battery overdischarging	Level 2	Weibull	10^{-5}	2	447
Battery internal short circuit	Level 4	Weibull	10^{-9}	2	44721
Internal wiring damage	Level 1	Weibull	10^{-3}	2	45
<i>Propulsion Subsystem</i>					
PMS failure	Level 2	Weibull	10^{-5}	2	447
Motor overheating	Level 2	Weibull	10^{-5}	2	447
Inverter overheating / short circuit	Level 3	Weibull	10^{-7}	2	4472
Rotor bird strike	Level 2	Weibull	10^{-5}	1	10,000
External wiring damage	Level 1	Weibull	10^{-3}	2	45

3. Component Sub-Net

Failure triggers and the effects of different interventions are captured at the component-level sub-net. Figure 8 provides an example of the battery sub-net corresponding to the configuration of eVTOL A with a total of six batteries, specifically for the internal short circuit failure mode. For better visualization, the sub-net is broken down into three sub-layers to show the individual paths that can be taken by the tokens under three different conditions. In other words, these three sub-layers are in reality merged into a single sub-net. A baseline value of $\beta = 2$ is used for the shape

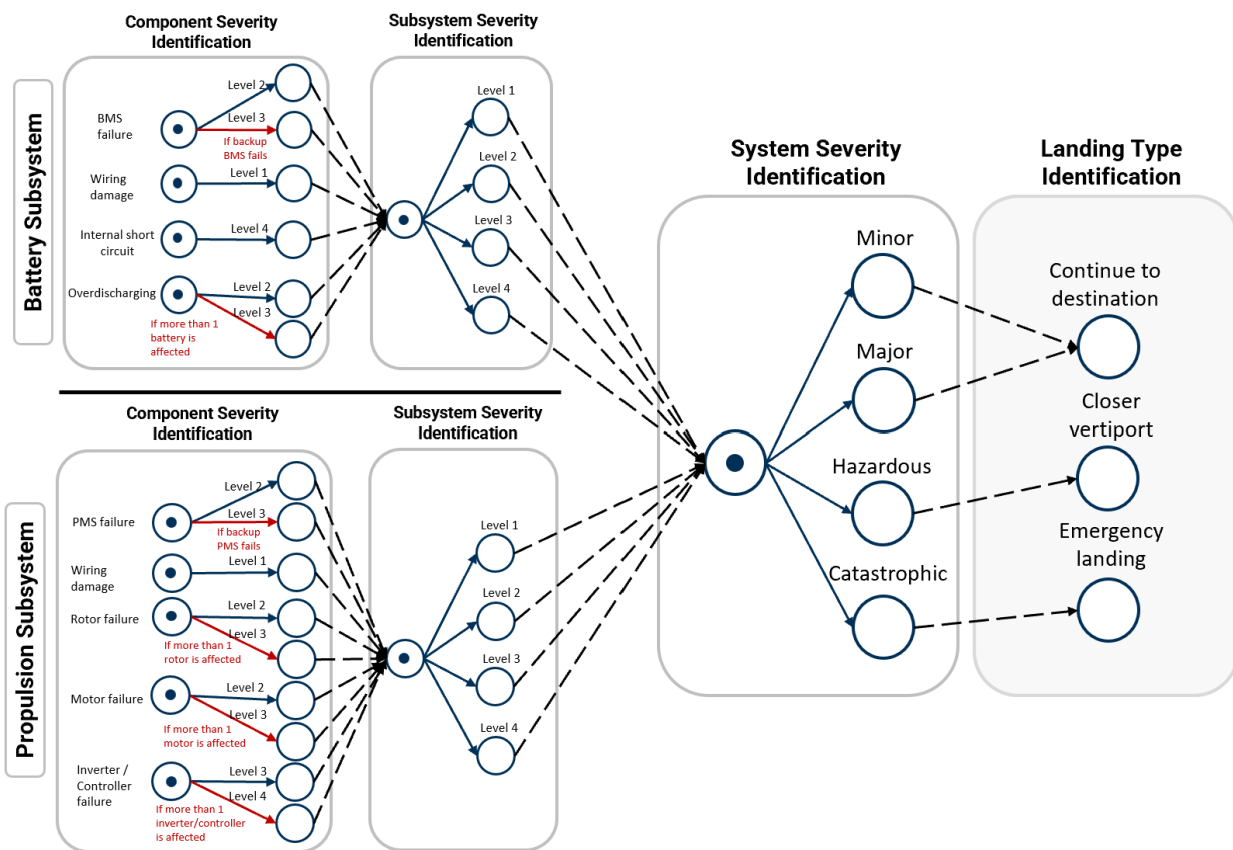


Fig. 7 Cascading of failure severity and eVTOL landing type identification

parameter to describe the behavior of all failure rates over time except for the rotor bird strike failure mode. Since this value is larger than 1, it represents an increasing failure rate with time, which is typically the case for wear-out failures such as mechanical and thermal aging. In contrast, the likelihood of a bird hitting one of the rotors is considered a random event. Consequently, the failure rate of this event is constant with time, hence $\beta = 1$. The allocated failure rate and shape parameter are substituted in Eq. 1 to determine the corresponding scale parameter for each failure mode as shown in Table 7. These two parameters are used to set the Weibull distribution for the failure likelihood of each individual component.

As previously mentioned, Fig. 8 decomposes the battery sub-net into three layers to provide better visualization of the different token paths governed by the conditioning of the transitions. Whenever the battery replacement counter reaches its threshold, all tokens corresponding to the battery packs in Fig. 8a are completely replaced, and their tokens' ages are reset to zero. As shown in Fig. 8b, if the system is due for scheduled maintenance, all battery tokens are pushed to the "scheduled repair" place where the tokens spend their allocated time under scheduled repair that is set to 8 hours for all eVTOL components. Upon completion, each token's age is multiplied by a factor of 0.85, reverting their age to 85% of their original value prior to undergoing scheduled maintenance. Should a failure or multiple failures occur during flight, the corresponding tokens are pushed to the corresponding failure mode place, (e.g., "Internal short circuit" place in Fig. 8c). This leads to the affected tokens being pushed to the "unscheduled repair" place right after landing and disembarkation of passengers. The failed components undergo failure diagnosis, repair whose time depends on the failure type and the number of failures, then recovery, after which each token's age is reverted to 95% of its original value, as indicated in Table 6. It should be noted that multiple layers of connectors, including inhibitors and enablers, are used across all sub-nets to ensure correct synchronization of events and continuous communication of status information between the tokens across the system, subsystem, and component levels without having them physically cross between sub-nets. For a simplified visualization of the model's building blocks, these interconnections are hidden.

VII. Results

This section presents the results obtained by comparing different metrics across three vehicle configurations. The analysis provides insight on how the failure occurrences, time metrics, and maintenance activities are affected by the system architecture and serves as a means to support the selection of more operationally efficient designs. The reliability performance of the three eVTOL configurations is evaluated using time metrics, failure analysis, severity assessment, and landing outcomes. It is important to note that these results are driven by all the assumptions made during the modeling process.

A. Reliability Time Metrics

The reliability time metrics for all three configurations exclude any ground time and only include flight time hours. The eVTOL mission lasts for about 10.8 minutes, or 0.18 hours, regardless of whether the vehicle is landing at its destination, to a closer vertiport, or conducting an emergency landing. Table 8 presents the MFOP, MTBF and MTTF metrics based only on flight time for each configuration. It is seen that eVTOLs B and C have a slightly longer MTTF compared to eVTOL A, with eVTOL B showing approximately 12% longer time to failure and eVTOL C showing 8% longer time to failure. In terms of MTBF, eVTOL B has the highest MTBF, indicating fewer failures per flight hour, followed by eVTOL C, then eVTOL A. The MFOP values are the lowest overall among the three metrics for all configurations, as MFOP accounts for both failure and scheduled maintenance activities. MFOP values range from 12.8 to 13.8 hours, which corresponds to approximately 71 to 76 missions before the occurrence of an operational interruption. By analyzing these metrics relative to the 0.18-hour mission duration, it is clear that all configurations have a high number of failure-free flights, with configuration B performing better overall, followed by configuration C, then configuration A.

Figure 9 presents the flight time and total downtime breakdown for the three eVTOL configurations. Across all three configurations, the flight time constitutes approximately 79.2% to 79.6% of total operation time, while total downtime accounts for 20.4% to 20.8%. When breaking down the total downtime, about 14% is due to planned maintenance, while the unplanned downtime resulting from failure occurrences, ranges from 6.4% to 6.9%. As proportion of total downtime, unplanned downtime represents roughly 31.2% to 32.9% with eVTOL B having the lowest proportion, which suggests a slightly better maintainability. Overall, all three configurations demonstrate similar operation time, with the majority of downtime due to planned maintenance activities.

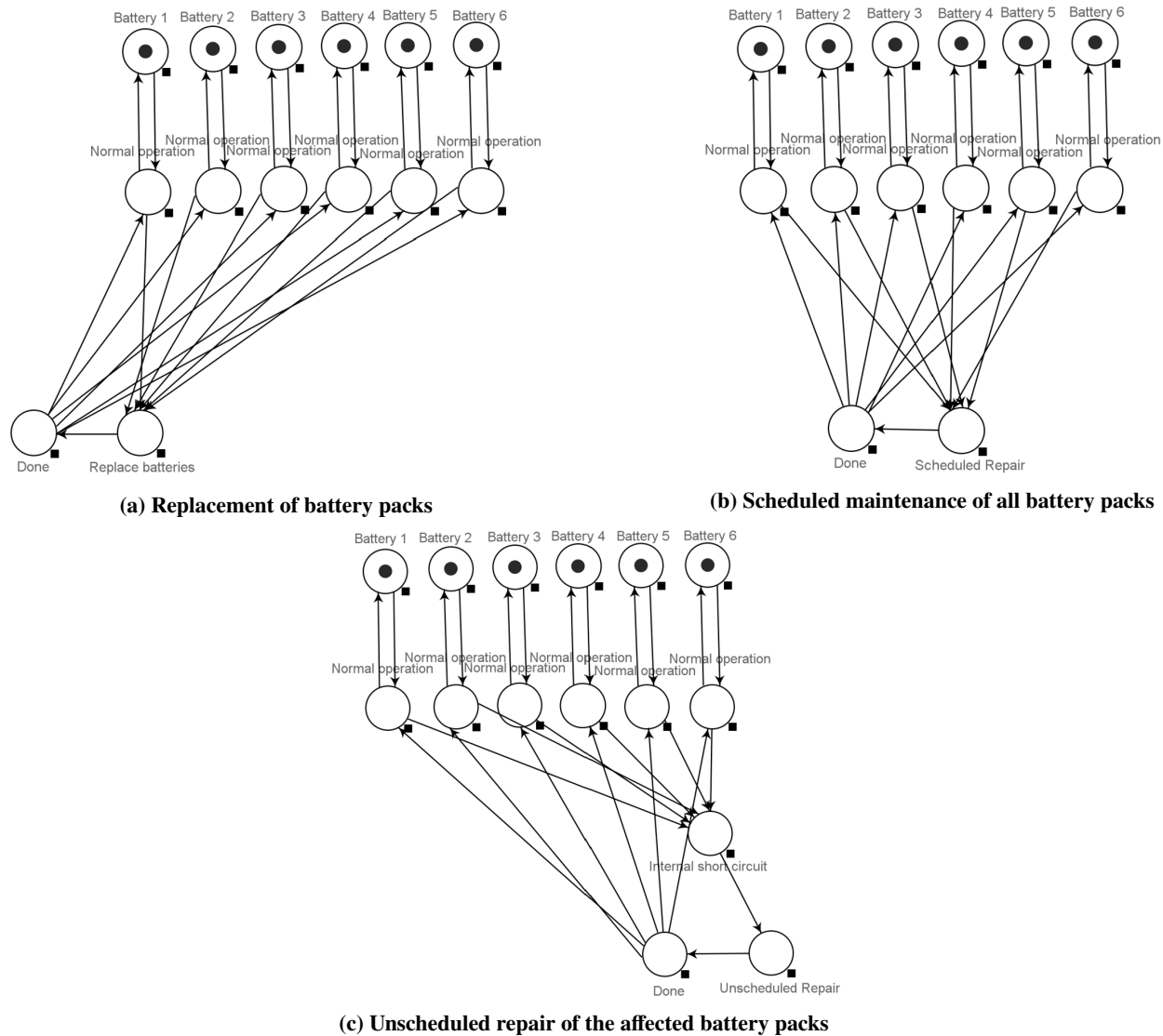


Fig. 8 Breakdown of the battery pack component-level sub-net of the battery subsystem

Table 8 Reliability time metrics comparison

Configuration	MTTF (h)	MTBF (h)	MFOP (h)
eVTOL A	17.73	17.81	12.78
eVTOL B	19.79	19.86	13.80
eVTOL C	19.19	19.28	13.52

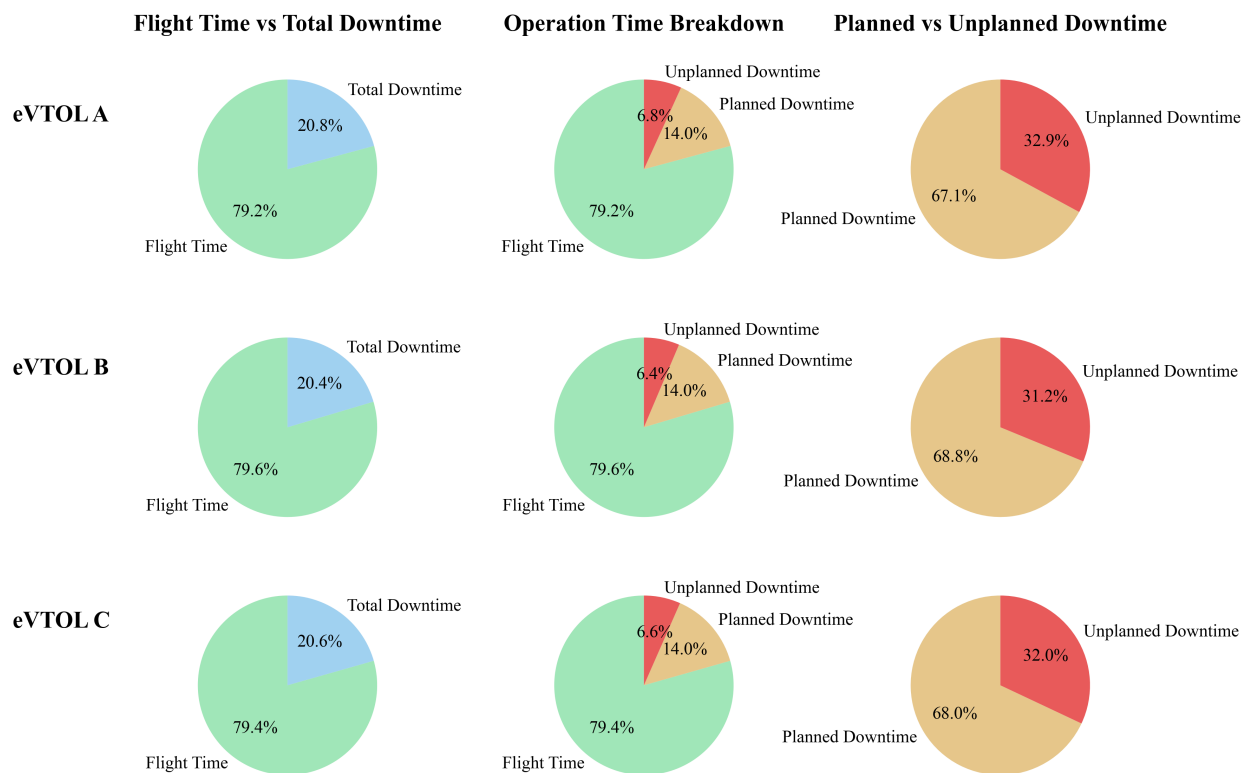


Fig. 9 Flight time and total downtime breakdown

B. Failures, Severity Level and Landing Outcomes

The total number of subsystem failures across the three configurations is compared using raw versus normalized values. Figure 10 shows the raw failure counts for each eVTOL. It is seen that configuration A has the highest number of failures in the battery subsystem, and configuration C reports the highest number of propulsion subsystem failures. However, these values only reflect the total number of failures and do not take into account the different architectures of eVTOLs. To gain insight on how the architecture affects subsystem reliability, the data was normalized by the number of rotors and batteries corresponding to each architecture. This normalization enables a functional-level comparison of failure events. The results depicted in Fig. 11 show that configuration A, despite having the highest number of battery failures, reports the lowest failure count when normalized. Conversely, Configuration B, which had the lowest number of failures in the raw data, reports the highest normalized failure counts in both subsystems. This suggests that as the number of batteries or rotors decreases, the failure count per component increases, which impacts the overall system reliability. Therefore, system architecture and component redundancy play a significant role in functional reliability.

Figure 12 presents the severity levels of subsystem failures for eVTOL A. The complete data for all three configurations contained in Appendix A show a consistent trend for both battery and propulsion subsystems. The battery subsystem is mainly composed of Level 1 and 2 severity failures across all three vehicles. On the other hand, the propulsion subsystem consists of Level 1, 2, and 3 failures across all three configurations. Notably, no Level 4 failures are observed in either subsystem. This indicates that while the eVTOLs experience a range of failure severities, Level 3 events occur less frequently than Level 1 and Level 2 events and are confined to the propulsion subsystem, whereas Level 4 events are absent from both subsystems.

Figure 13 provides a component-level breakdown of subsystem failures for eVTOL A. The complete data for all three configurations contained in Appendix B show a clear trend in frequency and severity level. Across all configurations, the wiring failures for both the battery and propulsion subsystems dominate and account for the highest number of failures observed. However, the severities of these failures are classified as Level 1. BMS and PMS failures are the next most significant contributors to failures, followed by battery overdischarge, all of which fall under a severity of Level 2. While Level 1 and Level 2 failures make up the majority of reported failures, Level 3 failures occur at significantly lower frequencies. Additionally, the failure rates per component are consistent across the different configurations, with all of them not reporting any catastrophic failure.

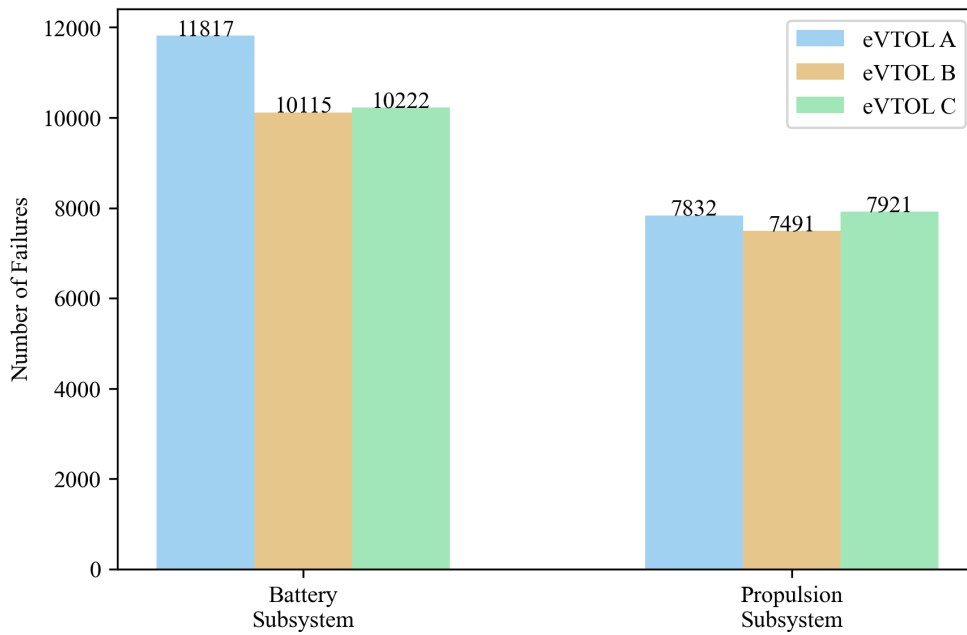


Fig. 10 Number of total failures per subsystem

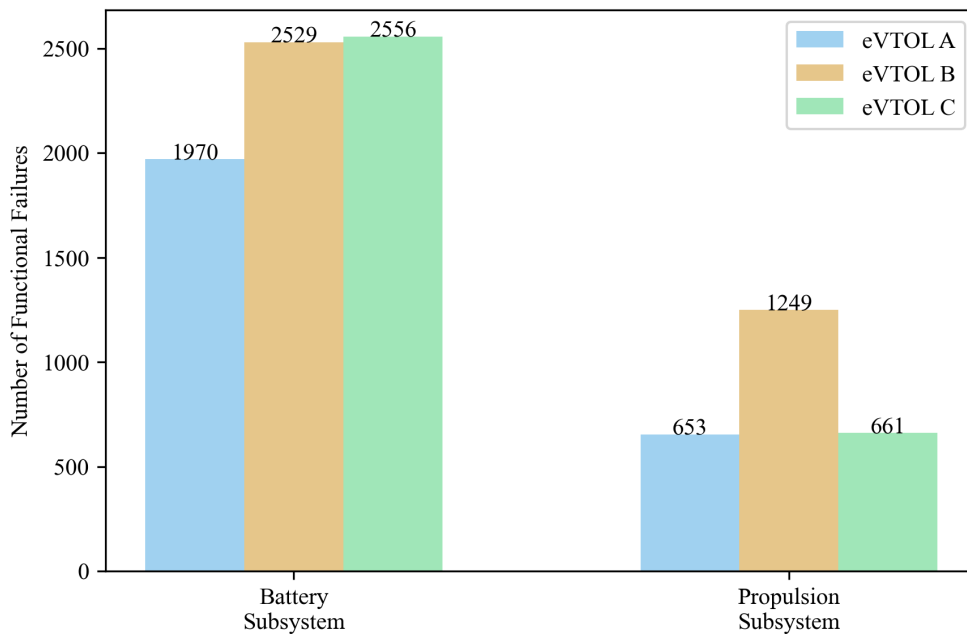


Fig. 11 Normalized number of total failures per subsystem



Fig. 12 eVTOL A Subsystem failure severity levels

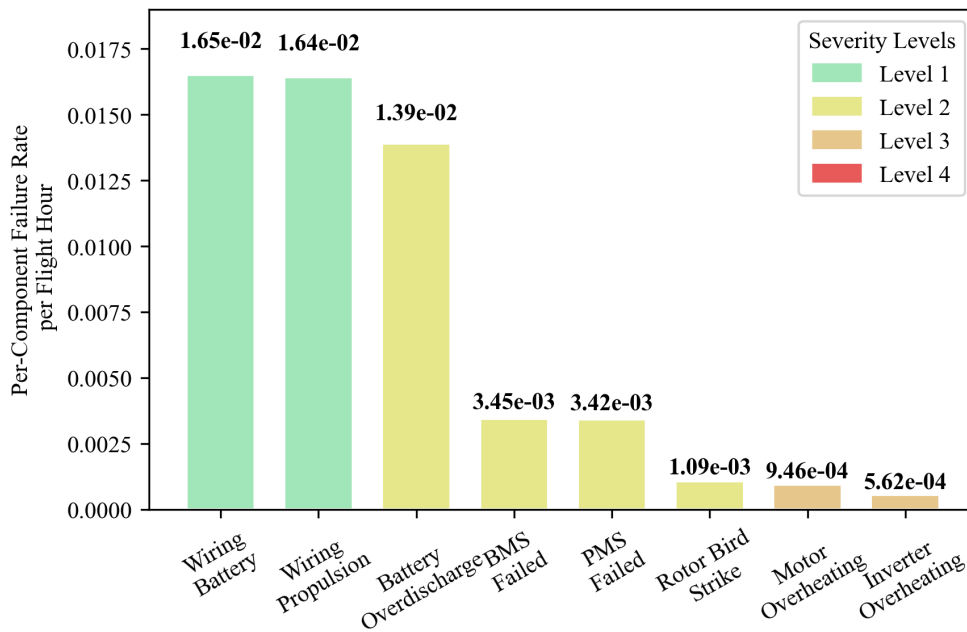


Fig. 13 eVTOL A Component failure severity levels

Figure 14 illustrates the landing scenarios, which demonstrate high operational reliability across all eVTOL configurations. Among flights that experienced failures, 97.0% to 98.3% successfully landed at their destinations. It is seen that eVTOL B has the highest mission completion rate followed by eVTOL A. On the other hand, flights that diverted to a closer vertiport account for 1.7% to 3.0% of the total scenarios, with configuration C having the highest number of redirected flights. Emergency landings were not observed for any of the configurations due to the absence of catastrophic failure events.

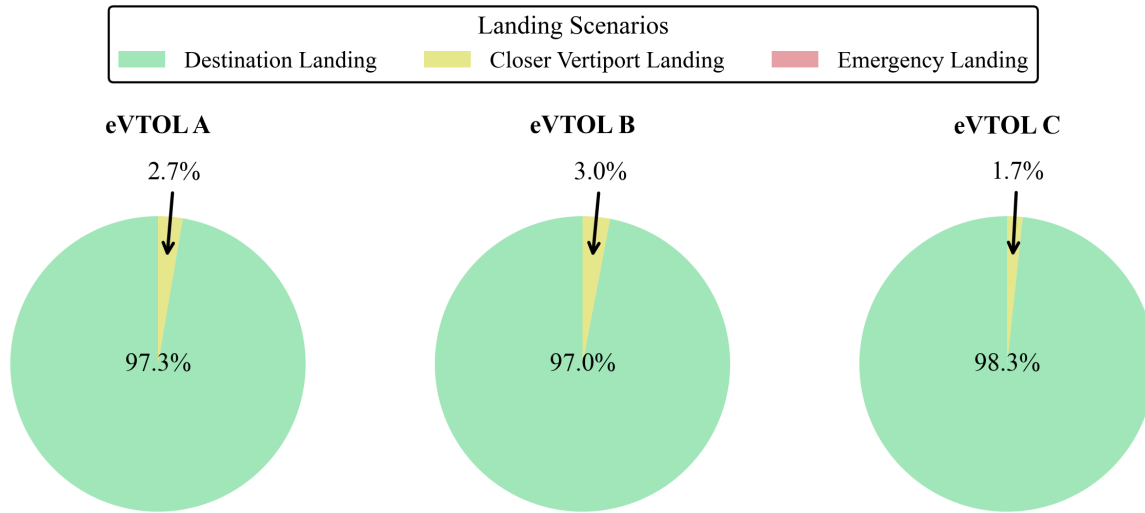


Fig. 14 Breakdown of landing scenarios

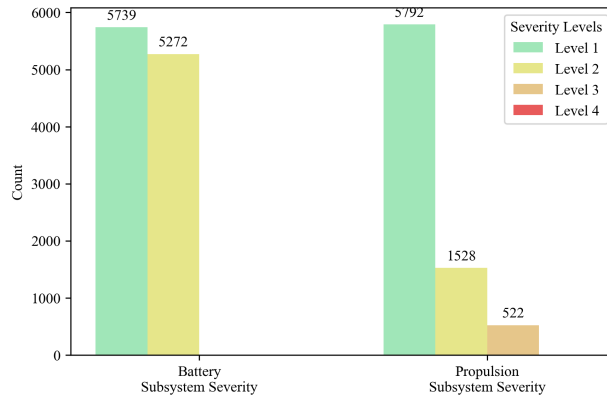
The operational reliability assessment demonstrates that while the difference in architecture influences the functional-level failures, the three configurations maintain a similar overall reliability performance. This shows that the methodology can be used to compare different configurations and effectively distinguish between component-level architecture effects and overall mission reliability.

VIII. Conclusion

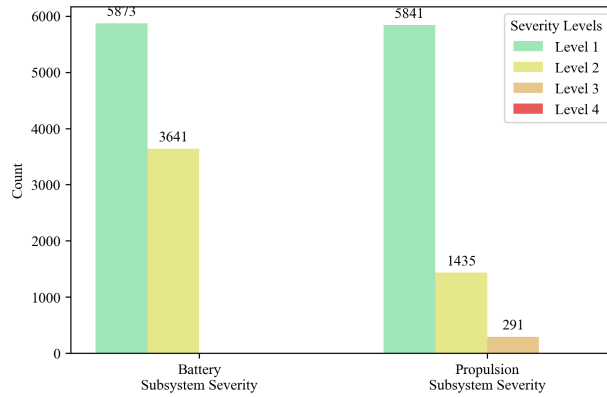
This paper proposes a comprehensive parametric methodology for assessing the operational reliability of eVTOL aircraft to enable more efficient maintenance planning and risk reduction. The methodology is demonstrated by comparing three different eVTOL configurations to show how it can provide insights for evaluating the overall system reliability and supporting operational decision making. While the developed model is not currently based on real-world data, it can be calibrated to enhance the relevance and applicability of the generated insights, contingent on access to the appropriate datasets. The comparison of the three configurations using the proposed methodology showed that eVTOL aircraft maintain high operational reliability, with more than 97% flights landing at destinations and no emergency landings observed. Additionally, it demonstrated how the differences in architectures influence functional-level failures while maintaining a consistent overall mission reliability across the three configurations. This shows that component redundancy helps mitigate architecture-related failures, as well as providing insight into how design choices affect individual component reliability while maintaining overall reliability. Additionally, the time-based metrics show that the configurations complete about 71 to 77 successful missions before encountering a failure or requiring scheduled maintenance. Such insights can help operators develop efficient preventive and corrective maintenance strategies. By enabling systematic comparison of different vehicle configurations, the proposed methodology supports informed decision making that enables efficient maintenance planning, extends component service life, and minimizes operational risks.

Appendix A. Subsystem Failure Severity Levels

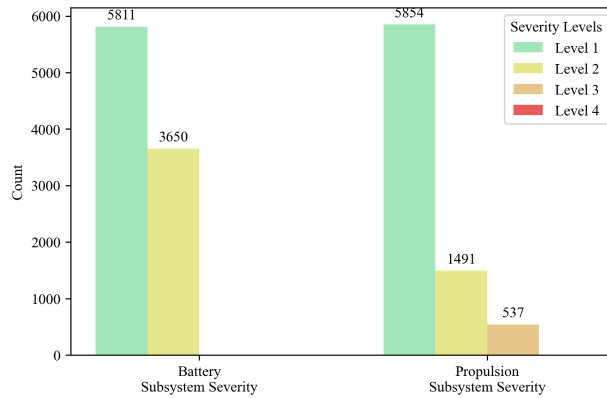
Figure 15 presents the distribution of subsystem failure severity levels (Levels 1–4) for battery and propulsion subsystems across eVTOL A, B, and C.



(a) eVTOL A



(b) eVTOL B

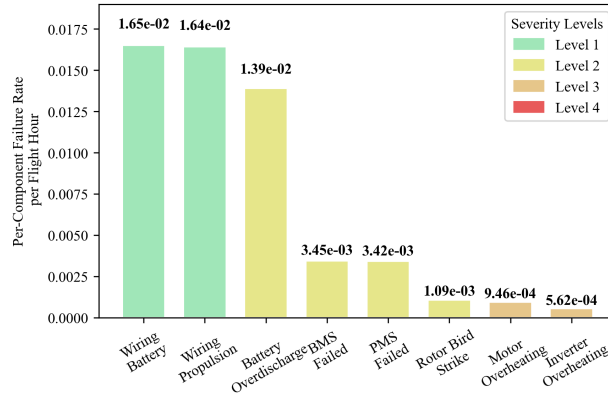


(c) eVTOL C

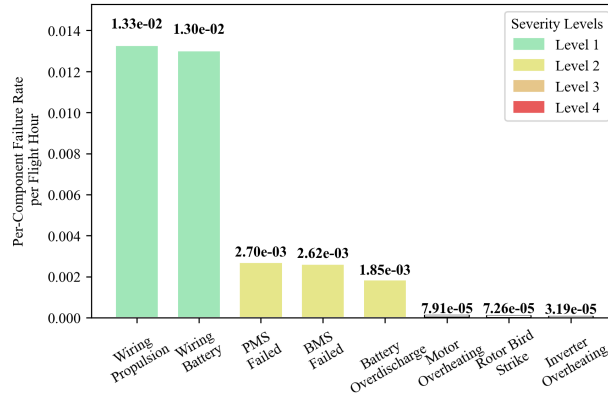
Fig. 15 Subsystem failure severity levels (Levels 1–4) for battery and propulsion systems in eVTOL A, B, and C

Appendix B. Component Failure Severity Levels

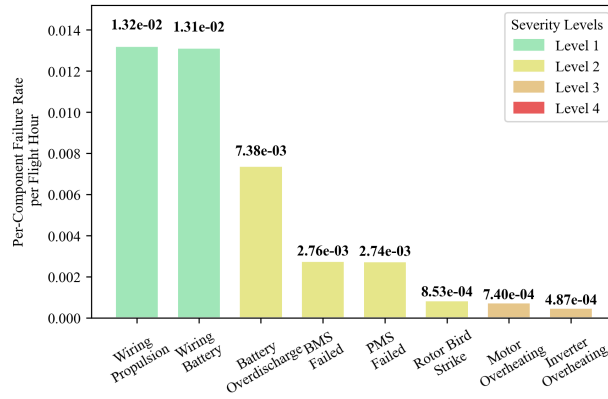
Figure 16 presents the distribution of component failure severity levels (Levels 1–4) for battery and propulsion subsystems across eVTOL A, B, and C.



(a) eVTOL A



(b) eVTOL B



(c) eVTOL C

Fig. 16 Component failure severity levels (Levels 1–4) for battery and propulsion systems in eVTOL A, B, and C

References

- [1] Raigoza, K., Chadwick, A., and Kishore, C., “Electric Vertical Take-Off and Landing (eVTOL) Vehicle Reliability and Safety Analysis,” American Society of Mechanical Engineers, Columbus, Ohio, USA, 2022. <https://doi.org/10.1115/IMECE2022-97038>.
- [2] Kinjo, H., “Development trends and prospects for eVTOL: a new mode of air mobility,” 2018. URL https://www.mitsui.com/mgssi/en/report/detail/_icsFiles/afieldfile/2019/07/18/1906m_kinjo_e.pdf.
- [3] Su, J., Huang, H., Zhang, H., Wang, Y., and Wang, F.-Y., “eVTOL Performance Analysis: A Review From Control Perspectives,” *IEEE Transactions on Intelligent Vehicles*, Vol. 9, No. 5, 2024, pp. 4877–4889. <https://doi.org/10.1109/TIV.2024.3387405>.
- [4] Ugwueze, O., Statheros, T., Horri, N., Innocente, M., and Bromfield, M., “Investigation of a Mission-based Sizing Method for Electric VTOL Aircraft Preliminary Design,” *AIAA SCITECH 2022 Forum*, American Institute of Aeronautics and Astronautics, San Diego, CA & Virtual, 2022. <https://doi.org/10.2514/6.2022-1931>.
- [5] Liu, Y., and Wang, L., “High-Fidelity Simulations of Lift+Cruise VTOL Urban Air Mobility Concept Aircraft in Hover,” *AIAA SCITECH 2024 Forum*, American Institute of Aeronautics and Astronautics, Orlando, FL, 2024. <https://doi.org/10.2514/6.2024-1118>.
- [6] Rendón, M. A., Sánchez R., C. D., Gallo M., J., and Anzai, A. H., “Aircraft Hybrid-Electric Propulsion: Development Trends, Challenges and Opportunities,” *Journal of Control, Automation and Electrical Systems*, Vol. 32, No. 5, 2021, pp. 1244–1268. <https://doi.org/10.1007/s40313-021-00740-x>.
- [7] Cheng, Z., Cao, Z., Mi, C., and Hwang, J. T., “Cost Optimization of Electric Vertical Takeoff and Landing Aircraft Through Powertrain Modeling,” *Journal of Air Transportation*, 2025, pp. 1–12. <https://doi.org/10.2514/1.D0487>.
- [8] U.S. Helicopter Safety Team, “USHST Monthly Safety Report for Jan 2025,” , January 2025. URL <https://www.faasafety.gov/spans/noticeView.aspx?nid=14212>.
- [9] U.S. Helicopter Safety Team, “U.S. Helicopter Accident Rate Levels Off During 2017,” , Feb. 2018. URL https://ushst.org/Press_Releases/2017Full.pdf.
- [10] Saleh, J., Tikayat Ray, A., Zhang, K., and Churchwell, J., “Maintenance and inspection as risk factors in helicopter accidents: Analysis and recommendations,” *PLOS ONE*, Vol. 14, 2019, p. e0211424. <https://doi.org/10.1371/journal.pone.0211424>.
- [11] Volovoi, V., “Abridged Petri Nets,” 2020. URL <https://www.volovoi.com/publications.html>.
- [12] Wei, H., “Introduction of Reliability Engineering,” 2012. URL <https://www.slideshare.net/ASQwebinars/vreview-of-reliability-engineering>, accessed: June 5, 2025.
- [13] Rinne, H., *The Weibull Distribution: A Handbook*, 1st ed., Chapman and Hall/CRC, 2008. <https://doi.org/10.1201/9781420087444>.
- [14] Ahmadi, A., and Soderholm, P., “Assessment of Operational Consequences of Aircraft Failures: Using Event Tree Analysis,” *2008 IEEE Aerospace Conference*, 2008. <https://doi.org/10.1109/AERO.2008.4526622>.
- [15] SAE International, “Guidelines and Methods for Conducting the Safety Assessment Process on Civil Airborne Systems and Equipment,” SAE ARP4761, Dec. 1996. <https://doi.org/https://doi.org/10.4271/ARP4761>.
- [16] Xu, M., and Wu, Y., “Evolutionary Maintenance Based on Maintenance Free Operating Period Philosophy,” *Procedia Engineering*, Vol. 99, 2015, pp. 587–592. <https://doi.org/10.1016/j.proeng.2014.12.575>.